

# The numerical solution of three-dimensional Signorini problems with the method of fundamental solutions

A. Poullikkas<sup>a</sup>, A. Karageorghis<sup>b,\*</sup>, G. Georgiou<sup>b</sup>

<sup>a</sup>Electricity Authority of Cyprus, P.O. Box 40113, 6301 Lamaca, Cyprus

<sup>b</sup>Department of Mathematics and Statistics, University of Cyprus, Kallipoleos 75, P.O. Box 20537, CY-1678 Nicosia, Cyprus

Received 11 July 2000; revised 13 November 2000; accepted 28 November 2000

Dedicated to the memory of Yiouli Poullikkas

## Abstract

The method of fundamental solutions (MFS) is formulated for three-dimensional Signorini boundary-value problems. The method is tested on a three-dimensional electropainting problem related to the coating of vehicle roofs. The numerical results are in good agreement with available numerical solutions. © 2001 Elsevier Science Ltd. All rights reserved.

*Keywords:* Method of fundamental solutions; Three-dimensional elliptic boundary-value problems; Signorini problems; Electropainting problem

*PACS:* 65N99

## 1. Introduction

The method of fundamental solutions (MFS) has become popular in recent years and has proven to be an excellent alternative to the standard boundary element method (BEM) for the numerical solution of certain elliptic boundary-value problems. The development of the MFS over the last three decades is the subject of a recent review article by Fairweather and Karageorghis [4].

The MFS is particularly effective when dealing with free boundary problems, since in these problems, one is interested primarily in the solution on the boundary. Further, the nonlinear nature of the MFS enables it to take into account the nonlinearities present in free boundary problems without great difficulty. The MFS was first applied to free boundary problems in Ref. [6], where problems from potential theory were considered. Poullikkas et al. [16] applied the MFS to a free boundary Stokes flow problem. Karageorghis and Fairweather [7] solved a free boundary problem, governed by the axisymmetric version of Laplace's equation.

Signorini-type problems form a special class of free boundary problems [3,5,6] and are the subject of a recent survey article by Howison et al. [5]. On part of the boundary, two types of condition alternate in conjunction with certain inequality constraints. The main difficulty in these

problems arises from the fact that the numbers and the positions of the points or curves where a change from one type of condition to the other occurs are unknown [18]. In boundary element methods, the determination of the locations of the boundary points or curves of change of the boundary conditions usually requires special iterative schemes [1,2,14]. As demonstrated by Poullikkas et al. [17], who applied the MFS to two-dimensional Signorini problems, the boundary inequalities in the MFS can be incorporated directly into the minimization scheme and thus the need to design iterative algorithms is avoided.

Despite the popularity of the MFS and its successful application to a large variety of physical problems over recent years, its mathematical foundation has been investigated only for certain harmonic Dirichlet problems when fixed singularities are used. In particular, in Refs. [8,11], it is shown that, when the method is applied to a harmonic Dirichlet problem in a disk of radius  $r$  and the singularities are placed on a circle of radius  $R > r$ , then exponential convergence is achieved. In Refs. [9,10], this result is generalized to regions in the plane whose boundaries are analytic Jordan curves.

The objective of this work is to formulate the MFS for the solution of three-dimensional Signorini problems. To demonstrate the applicability of the method, we solve a potential problem, known as the electropainting problem [14], which is described in Section 2. This problem has been solved recently by Poole and Aitchison [14] using the boundary element method. The MFS formulation is

\* Corresponding author.

E-mail address: andreask@ucy.ac.cy (A. Karageorghis).

described in Section 3. In Section 4, we present our numerical results, which are found to agree well with those of Poole and Aitchison.

### 2. The electropainting problem

The electropainting problem describes the coating process of metal surfaces with paint [1,2]. Aitchison et al. [1] formulated the two-dimensional version of this problem as a Signorini problem and solved it using a finite element method. Poullikkas et al. [17] also solved this two-dimensional problem using the MFS and obtained similar results. The three-dimensional electropainting problem is described in detail in a recent paper by Poole and Aitchison [14], where the problem was modeled and solved with the boundary element method combined with iterative algorithms.

Physically, the car body shells are attached to a large hoist, which lowers them into the bath containing the electrolyte solution. In practice, the values of both the critical current  $\epsilon$  and the height  $h$  of the solution above the car roof, must be chosen carefully in order to obtain an even distribution over the whole roof. To model the car roof and the volume of the electrolyte, the cuboid  $\Omega$  of Fig. 1 is used. The problem is formulated as a Signorini problem for the

electric potential  $\phi$  in the paint solution [14]. In steady state, the governing equation is:

$$\nabla^2 \phi = 0 \text{ in } \Omega = (-\alpha, \alpha) \times (-h/2, h/2) \times (-\beta, \beta). \quad (1)$$

The face  $S_1$  of the cuboid  $\Omega$  (shown in Fig. 1) is the surface of the electrolyte solution with insulating air above it. Hence

$$\frac{\partial \phi}{\partial n} = 0 \text{ on } S_1. \quad (2)$$

The anode consists of the sides  $S_2, S_3, S_4$  and  $S_5$ , where the voltage  $V$  is applied so that

$$\phi = V \text{ on } S_2 \cup S_3 \cup S_4 \cup S_5. \quad (3)$$

Finally, the face  $S_6$  is the car roof to be painted, which is the cathode. On this surface, the parts that are painted are not known a priori. On the unpainted subregions of  $S_6$ , the boundary conditions are

$$\phi = 0, \quad \frac{\partial \phi}{\partial n} + \epsilon > 0, \quad (4)$$

while on the painted ones

$$\frac{\partial \phi}{\partial n} + \epsilon = 0, \quad \phi > 0. \quad (5)$$

Eq. (1) and boundary conditions (2)–(5) constitute a

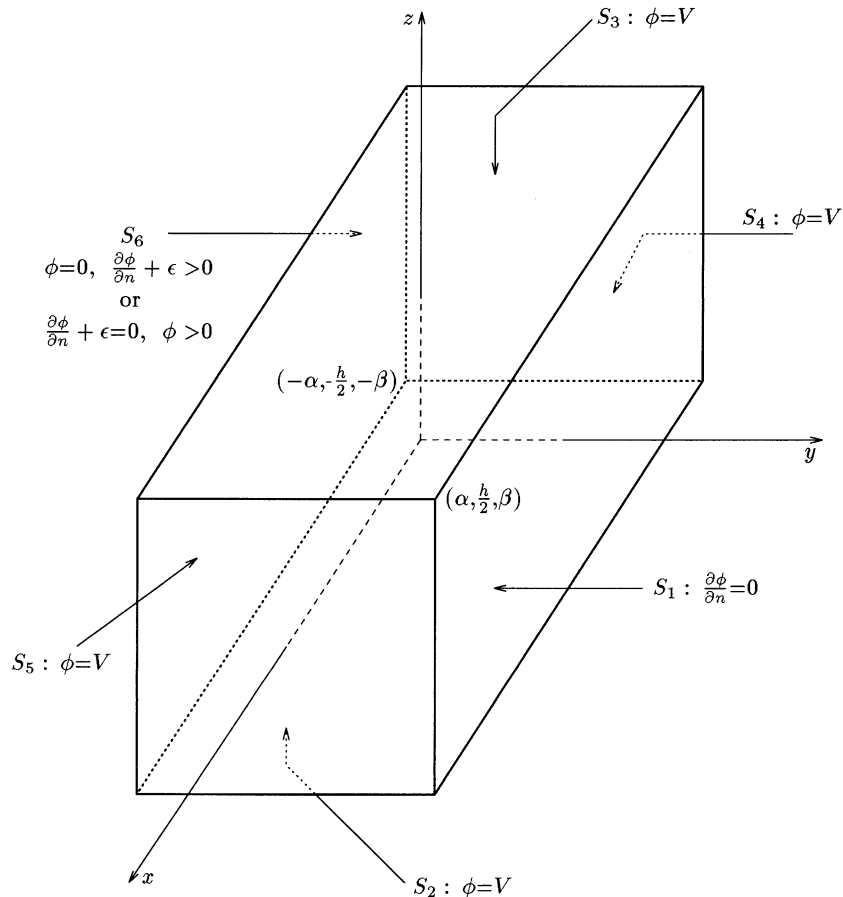


Fig. 1. Geometry and boundary conditions of the electropainting problem.

Table 1

Convergence of the solution with  $\tau$ ;  $0.1 \times 0.1$  grid near the car roof center,  $h = 0.05$ ,  $\epsilon = 6$  and  $N = 6$

(0,0)				
0.05995	0.04611	0.03482	0.02681	0.02264
0.05168	0.03049	0.01499	0.00501	0.00000
0.05165	0.03038	0.01495	0.00493	0.00000
0.05165	0.03038	0.01495	0.00493	0.00000
(0,0)				
0.06369	0.06021	0.05924	0.03146	0.02742
0.05423	0.03367	0.01888	0.00914	0.00489
0.05415	0.03361	0.01876	0.00911	0.00483
0.05415	0.03361	0.01876	0.00911	0.00483
(0,0)				
0.06089	0.05810	0.04771	0.04036	0.03654
0.05945	0.04038	0.02666	0.01778	0.01346
0.05939	0.04035	0.02663	0.01776	0.01341
0.05939	0.04035	0.02663	0.01776	0.01341
(-0.4,-0.2)				

$\tau = 10^{-2}$
$\tau = 10^{-3}$
$\tau = 10^{-4}$
$\tau = 10^{-5}$
$\tau = 10^{-6}$

harmonic Signorini boundary-value problem. In order to obtain conditions valid everywhere on  $S_6$ , one can combine conditions (4) and (5) as follows:

$$\phi \geq 0, \quad \frac{\partial \phi}{\partial n} + \epsilon \geq 0 \quad \text{and} \quad \phi \left( \frac{\partial \phi}{\partial n} + \epsilon \right) = 0 \quad \text{on} \quad S_6. \quad (6)$$

Compared to the other length scales of the problem, the paint thickness, which is defined as  $\phi/\epsilon$ , is very small [14].

### 3. Formulation of the MFS

In the MFS, the solution  $\phi$  is approximated by a set of fundamental solutions of the governing equation, which are expressed in terms of sources located outside the domain  $\Omega$  [12]. We use  $N$  sources, the positions of which are unknown; these are calculated as part of the solution. On the boundary, we place  $M$  fixed points  $\mathbf{p}_i$ . Let  $\mathbf{t}_j = (t_{j_x}, t_{j_y}, t_{j_z})$  denote the coordinates of source  $j$  and  $\mathbf{p}_i = (p_{i_x}, p_{i_y}, p_{i_z})$  be the coordinates of boundary point  $i$ . The solution  $\phi_i$  at the point  $\mathbf{p}_i$  is approximated by

$$\bar{\phi}_i = \bar{\phi}(\mathbf{c}, \mathbf{t}, \mathbf{p}_i) = \sum_{j=1}^N c_j k(\mathbf{t}_j, \mathbf{p}_i), \quad (7)$$

where  $k(\mathbf{t}_j, \mathbf{p}_i) = r_{ij}^{-1}$  is the fundamental solution of Laplace's equation in three dimensions with  $r_{ij}$  being the distance between boundary point  $i$  and the source  $j$ , i.e.

$$r_{ij} = \sqrt{(p_{i_x} - t_{j_x})^2 + (p_{i_y} - t_{j_y})^2 + (p_{i_z} - t_{j_z})^2}.$$

The vectors  $\mathbf{c} = [c_1, c_2, \dots, c_N]^T$  and  $\mathbf{t} = [t_{1_x}, t_{1_y}, t_{1_z}, t_{2_x}, t_{2_y}, t_{2_z}, \dots, t_{N_x}, t_{N_y}, t_{N_z}]^T$  contain the unknown coefficients of the fundamental solutions and the unknown coordinates of the sources, respectively. Hence, the total number of unknowns is  $4N$ . The positions of the  $M$  fixed boundary points and the initial location of the  $N$  moving sources are important factors in the least squares procedure. The boundary points are distributed uniformly on the boundary. In this application of the MFS, extensive experimentation indicated that approximately  $6N^2$  boundary points were required for the optimal representation of the boundary.

Since  $\bar{\phi}$  is a solution of the governing equation (1), the unknowns are determined so that the boundary conditions are satisfied in a least squares sense. This is achieved by

minimizing the functional

$$F(\mathbf{c}, \mathbf{t}) = \sum_{i=1}^{M_1} \left( \frac{\partial \bar{\phi}_i}{\partial n} \right)^2 + \sum_{i=M_1+1}^{M_1+M_2+M_3+M_4+M_5} (\bar{\phi}_i - 1)^2 + \sum_{i=M_1+M_2+M_3+M_4+M_5+1}^M \left[ \bar{\phi}_i \left( \frac{\partial \bar{\phi}_i}{\partial n} + \epsilon \right) \right]^2, \tag{8}$$

subject to the following three inequality constraints:

$$\bar{\phi} \geq 0, \text{ on } S_6, \tag{9}$$

$$\frac{\partial \bar{\phi}}{\partial n} + \epsilon \geq 0 \text{ on } S_6, \tag{10}$$

and

$$\max \left( \frac{|x|}{\alpha}, \frac{2|y|}{h}, \frac{|z|}{\beta} \right) > 1.0, \tag{11}$$

where  $M_i$  denotes the number of boundary points on  $S_i$ ,  $i = 1, 2, \dots, 6$ . The nonlinear constraint (11) ensures that the sources remain outside the domain. It should be emphasized that enforcing the inequality constraints (9)–(11) is accom-

modated directly in the minimization scheme and that the total number of unknowns is not altered.

The minimization of the nonlinear functional  $F$ , subject to the inequality constraints (9)–(11), is carried out using the least squares subroutine E04UPF of the NAG Library [13]. This routine is designed to minimize an arbitrary sum of squares subject to constraints, such as simple bounds on the variables, linear constraints, and nonlinear constraints. The user is required to supply the least squares subroutine with an initial estimate of the solution, which in this case depends on the initial locations of the singularities in the MFS expansion. Usually, the singularities are placed uniformly around the domain of the problem at a fixed distance  $d$  from the boundary (see Ref. [15]). The least squares subroutine E04UPF terminates when either a user-specified tolerance  $\tau$  is achieved or a user-specified maximum number of iterations NITER is reached. Thus, the user specifies either  $\tau$  or NITER. In this study, we specified  $\tau$ . Clearly, the tolerance one specifies depends on the accuracy required by the user. Usually, the tolerance is taken to be at least of order  $10^{-5}$ . The results of Table 1 indicate that this value of the tolerance ensures convergence of the results up to at least five decimal digits. The user must also supply subroutines that define the functions and the nonlinear constraints. If the exact Jacobian is not provided by the

Table 2  
Convergence of the solution with  $N$ ;  $0.1 \times 0.1$  grid near the car roof center,  $h = 0.05$ ,  $\epsilon = 6$  and  $\tau = 10^{-6}$

(0,0)				
0.05274	0.03115	0.01399	0.00432	0.00000
0.05205	0.03088	0.01458	0.00486	0.00000
0.05187	0.03054	0.01463	0.00491	0.00000
0.05165	0.03038	0.01495	0.00493	0.00000
0.05165	0.03038	0.01495	0.00493	0.00000
0.05547	0.03465	0.01946	0.01067	0.00443
0.05489	0.03401	0.01902	0.01032	0.00460
0.05436	0.03379	0.01896	0.00955	0.00465
0.05415	0.03361	0.01876	0.00911	0.00483
0.05415	0.03361	0.01876	0.00911	0.00483
0.06099	0.04174	0.02774	0.01861	0.01467
0.06007	0.04132	0.02718	0.01809	0.01434
0.05982	0.04067	0.02689	0.01793	0.01380
0.05939	0.04035	0.02663	0.01776	0.01341
0.05939	0.04035	0.02663	0.01776	0.01341
(-0.4,-0.2)				

$N = 4, M = 96$
$N = 5, M = 150$
$N = 6, M = 216$
$N = 7, M = 294$

user, it is approximated internally by finite differences. More details concerning the use and performance of the subroutine E04UPF in the MFS context can be found in Ref. [17].

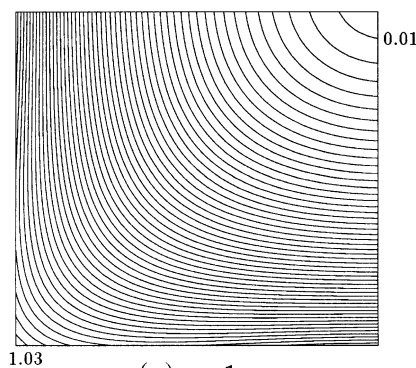
#### 4. Numerical results and discussion

In order to make comparisons with the numerical results of Poole and Aitchison [14], we consider the paint distribution on the roof of a car with dimensions  $\alpha = 0.75$  and  $\beta = 0.7$ . The sources were initially placed outside the domain at a distance  $d = 0.1$  from the boundary.

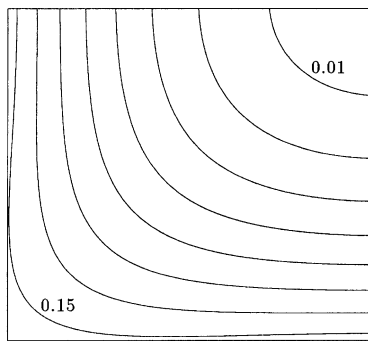
In Tables 1 and 2, we demonstrate the convergence of the MFS approximation with the tolerance  $\tau$  and the number of

sources  $N$ , respectively. In both tables, the solution is tabulated on a  $(0.1 \times 0.1)$  grid near the car roof center. In Table 2, we present values obtained for various values of  $N$  with  $\tau = 10^{-6}$ ; in Table 1, we present values obtained for various values of  $\tau$  with  $N = 6$ . We note that the numerical solution converges as  $N$  is increased and  $\tau$  is reduced. The results for  $N = 6$  and  $\tau = 10^{-5}$  have converged up to five decimal digits.

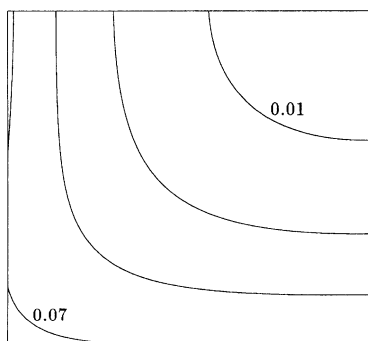
In Fig. 2, we present the paint distribution over the quarter of the car roof (which is sufficient because of symmetry), calculated for different values of  $\epsilon$  with  $h = 0.05$ ,  $N = 6$  and  $\tau = 10^{-6}$ . The paint thickness contours are plotted with a step of 0.01; the contour values increase as one moves from the upper right-hand corner, which corresponds to the center of the car roof, to the lower left-hand corner. Evidently,



(a)  $\epsilon=1$

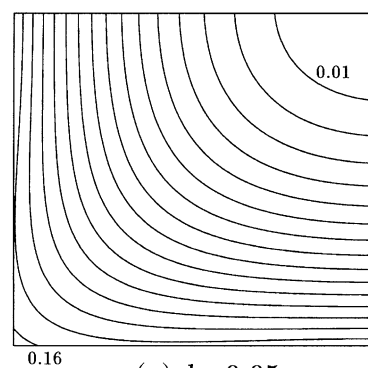


(b)  $\epsilon=6$

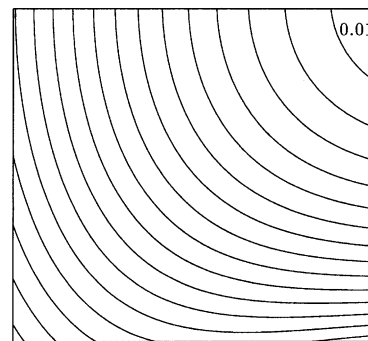


(c)  $\epsilon=12$

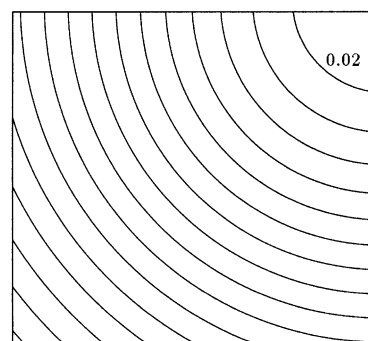
Fig. 2. Car roof paint distribution for different values of  $\epsilon$ ,  $h = 0.05$ ,  $N = 6$ ,  $M = 216$  and  $\tau = 10^{-6}$ .



(a)  $h=0.05$



(b)  $h=0.10$



(c)  $h=0.15$

Fig. 3. Car roof paint distribution for different values of  $h$ ,  $\epsilon = 6$ ,  $N = 6$ ,  $M = 216$  and  $\tau = 10^{-6}$ .

Table 3  
CPU times for various values of  $M$  and  $\tau$

$N$	$M$	$\tau$	CPU time (s)
4	96	$10^{-2}$	220
		$10^{-3}$	422
		$10^{-4}$	589
		$10^{-5}$	706
		$10^{-6}$	1034
5	150	$10^{-2}$	244
		$10^{-3}$	807
		$10^{-4}$	1200
		$10^{-5}$	1397
		$10^{-6}$	2091
6	216	$10^{-2}$	1165
		$10^{-3}$	3249
		$10^{-4}$	5334
		$10^{-5}$	5901
		$10^{-6}$	7014
7	294	$10^{-2}$	8521
		$10^{-3}$	20555
		$10^{-4}$	23754
		$10^{-5}$	26118
		$10^{-6}$	27966

the minimum paint thickness occurs near the center of the car roof. It can be seen that as  $\epsilon$  is increased, the paint thickness over the center of the roof decreases; at high values of  $\epsilon$ , the center of the roof remains unpainted. For small values of  $\epsilon$ , the car roof is completely painted with the center receiving the least amount of paint, as shown in Fig. 2(a), where we plot the results for  $\epsilon = 1$ . If we increase the value of  $\epsilon$ , the car roof center remains unpainted (Fig. 2(b)). Finally, at even higher values of  $\epsilon$ , the unpainted area becomes larger. These results are consistent with the qualitative results obtained for the corresponding two-dimensional case [1,17].

In Fig. 3, we show the paint distribution calculated for different values of  $h$  with  $\epsilon = 6$ ,  $N = 6$  and  $\tau = 10^{-6}$ . Again, the paint thickness contours are plotted with a step of 0.01. As before, the paint thickness decreases towards the center of the roof. We observe that, as  $h$  is increased, the paint thickness over the center of the car roof increases. For  $h = 0.05$ , the center of the roof remains unpainted, as shown in Fig. 3(a). If we increase the value of  $h$ , the roof center becomes painted (Fig. 3(b)) and at a higher value of  $h$ , the thickness of the paint near the roof center increases. These results are in good agreement with the only available results in the literature, i.e. those of Poole and Aitchison [14].

In order to solve Signorini-type problems using the conventional BEM, Poole and Aitchison [14] employ an iterative method, which is based on switching boundary conditions on boundary elements according to whether they correspond to the painted or the unpainted part of the boundary surface. This involves the solution of a sequence of linear systems, which are full. A more sophisticated switching algorithm is proposed by the same authors in Ref. [2]. In the case of the MFS, we solve a constrained

minimization problem, which is of comparable cost to solving a sequence of linear systems of the same order. In order to give an indication of the cost of the MFS solution of the problem, we present in Table 3 the CPU times required for certain numbers of degrees of freedom and values of the tolerance  $\tau$ . These were recorded on an IBM RS6000 (processor type: Power PC 604/100 MHz), for which the LINPACK TPP benchmark in MFLOPS is 56.4. Further, the application of the conventional BEM involves the potentially costly and troublesome evaluation of surface integrals, a feature that is absent from the MFS formulation. Also, the data preparation for the application of the MFS is minimal, involving only the boundary collocation points and the initial positions of the singularities rather than an elaborate surface discretization. For linear problems, it is true that the conventional BEM requires much less computational time than the MFS, as in the former, one needs to solve a linear system instead of carrying out nonlinear minimization. This is compensated partially by the ease of implementation associated with the MFS. Signorini-type problems (and free boundary problems in general) are nonlinear and the costs of the two methods are comparable as iterative techniques need to be used in conjunction with the conventional BEM.

We are presently investigating the extension of the present method for similar Signorini boundary-value problems occurring in elasticity, i.e. crack problems.

## Acknowledgements

The authors wish to thank Professor Graeme Fairweather of the Colorado School of Mines for his useful comments and suggestions and an anonymous referee for his/her constructive criticism.

## References

- [1] Aitchison JM, Lacey AA, Shillor M. A model for an electropaint process. *IMA J Appl Math* 1984;33:17–31.
- [2] Aitchison JM, Poole MW. A numerical algorithm for the solution of Signorini problems. *J Comput Appl Math* 1998;94:55–67.
- [3] Elliott CM, Ockendon JR. *Weak and variational methods for moving boundary problems*. London: Pitman, 1982.
- [4] Fairweather G, Karageorghis A. The method of fundamental solutions for elliptic boundary value problems. *Adv Comput Math* 1998;9:69–95.
- [5] Howison D, Morgan JD, Ockendon JR. A class of codimension two free boundary problems. *SIAM Rev* 1997;39:221–53.
- [6] Karageorghis A. The method of fundamental solutions for the solution of steady-state free boundary problems. *J Comput Phys* 1992;98:119–28.
- [7] Karageorghis A, Fairweather G. The method of fundamental solutions for axisymmetric potential problems. *Int J Numer Methods Engng* 1999;44:1653–69.
- [8] Katsurada M. A mathematical study of the charge simulation method II. *J Fac Sci, Univ Tokyo, Sect 1A, Math* 1989;36:135–62.
- [9] Katsurada M. Asymptotic error analysis of the charge simulation

- method in a Jordan region with an analytic boundary. *J Fac Sci, Univ Tokyo, Sect 1A, Math* 1990;37:635–57.
- [10] Katsurada M. Charge simulation method using exterior mapping functions. *Jpn J Ind Appl Math* 1994;11:47–61.
- [11] Katsurada M, Okamoto H. A mathematical study of the charge simulation method I. *J Fac Sci, Univ Tokyo, Sect 1A, Math* 1988;35:507–18.
- [12] Mathon R, Johnston RL. The approximate solution of elliptic boundary-value problems by fundamental solutions. *SIAM J Numer Anal* 1997;14:638–50.
- [13] Numerical Algorithms Group Library. Mark 16, NAG (UK) Ltd. Oxford: Wilkinson House, 1993.
- [14] Poole MW, Aitchison JM. Numerical model of an electropainting process with applications to the automotive industry. *IMA J Math Appl Bus Ind* 1997;8:347–60.
- [15] Poullikkas A, Karageorghis A, Georgiou G. Methods of fundamental solutions for harmonic and biharmonic boundary value problems. *Comput Mech* 1998;21:416–23.
- [16] Poullikkas A, Karageorghis A, Georgiou G, Ascough J. The method of fundamental solutions for Stokes flows with a free surface. *Numer Methods Partial Diff Eqns* 1998;14:667–78.
- [17] Poullikkas A, Karageorghis A, Georgiou G. The method of fundamental solutions for Signorini problems. *IMA J Numer Anal* 1998;18:273–85.
- [18] Spann W. On the boundary element method for the Signorini problem of the Laplacian. *Numer Math* 1993;65:337–56.